Available online at www.sciencedirect.com

SCIENCE DIRECT®

Journal of Molecular Catalysis A: Chemical 204–205 (2003) 545–552

JOURNAL OF MOLECULAR CATALYSIS A: CHEMICAL

www.elsevier.com/locate/molcata

AuPd bimetallic nanoparticles on TiO_2: XRD, TEM, in situ EXAFS studies and catalytic activity in CO oxidation

L. Guczi [a,*], A. Beck [a], A. Horváth [a], Zs. Koppány [a], G. Stefler [a], K. Frey [a], I. Sajó [b], O. Geszti [c], D. Bazin [d], J. Lynch [e]

[a] *Department of Surface Chemistry and Catalysis, Institute of Isotope and Surface Chemistry, Chemical Research Center (CRC), HAS, Konkoly Th. M. ut 29/33, P.O. Box 77, H-1525 Budapest, Hungary*

[b] *Institute of Chemistry, Chemical Research Center (CRC), HAS, P.O. Box 17, H-1525 Budapest, Hungary*

[c] *Institute of Technical Physics and Materials Science, HAS, P.O. Box 49, H-1525 Budapest, Hungary*

[d] *LURE, Université, Paris XI, Bât 209D, 91405 Orsay, France*

[e] *Institut Français du Pétrole, 1 & 4 Avenue de Bois Préau, 92852 Rueil-Malmaison, France*

Received 5 November 2002; received in revised form 17 March 2003; accepted 25 March 2003

Dedicated to Professor Renato Ugo on the occasion of his 65th birthday

Abstract

Monometallic Au, Pd and bimetallic AuPd nanoparticles were prepared from Au(III), Pd(II) precursor ions in aqueous media with reduction by a mixture of Na-citrate and tannin producing stable metal sols of narrow size distribution. The nanoparticles of 4–7 nm in diameter as indicated by transmission electron microscopy were adsorbed on TiO_2. In situ X-ray absorption spectroscopy (XAS) at Au L_{III} and Pd K-edges and X-ray diffraction (XRD) techniques evidenced the presence of bimetallic particles in the supported $AuPd/TiO_2$ sample. The high amount of organic residues of the samples was removed by calcination at 400 °C proved by temperature programmed oxidation (TPO). After reduction in H_2 the TEM, XRD and the CO chemisorption showed some enlargement in the metal particle sizes. The catalytic activity of the bimetallic $AuPd/TiO_2$ in the CO oxidation revealed a slight synergistic effect compared to the activity of monometallic analogous referred to the estimated surface area of Au and Pd in the bimetallic sample.

Keywords: Au/TiO_2; Pd/TiO_2; $AuPd/TiO_2$; TEM; XRD; EXAFS characterization; CO oxidation

1. Introduction

It is of great interest to study of gold-based nanoparticles due to their diverse range of physical [1,2] and catalytic properties [3–6]. Among the different parameters, which affect their activity/selectivity, the particle size, the nature of oxide supports (e.g. α-Fe_2O_3 [7], TiO_2 [8], SiO_2 [9] or ZrO_2 [10]) as well as the interaction between gold particles and the supporting oxide [11] can be mentioned. Particularly high activity of the gold nanoparticles in the CO oxidation is achieved by depositing gold on transition metal oxide of variable oxidation state. These oxides alone are generally also active catalysts providing activated oxygen to the CO oxidation. However, a combination with Au nanoparticles produces spectacularly high activity. According

* Corresponding author. Tel.: +361-392-2534; fax: +361-392-2703.
E-mail addresses: guczi@sunserv.kfki.hu, guczi@alpha0.iki.kfki.hu (L. Guczi).
URL: http://www.iki.kfki.hu/surcat/index.htm.

1381-1169/$ – see front matter © 2003 Elsevier B.V. All rights reserved.
doi:10.1016/S1381-1169(03)00337-6

to one of the explanations this is due to the increased number of oxygen vacancies responsible for O_2 activation in the oxides in vicinity of the gold/oxide interface [12]. The size of the Au particles being below 5 nm, plays a decisive role in the dramatic enhancements in the activity [13]. The formation and stabilization of such highly dispersed gold needs generally special preparation techniques.

Palladium on different supports is a well-known oxidation catalyst, on which the chemisorbed CO reacts with the subsurface oxygen. Combination of gold and palladium is an interesting possibility to achieve a catalyst with higher activity and to better understand the nature of the outstanding activity of gold containing catalysts. The exclusive effect of the co-operation of the two metals has been studied on inert silica support in CO oxidation because the promotional effect of the gold/silica interface was regarded negligible [14]. On silica Pd presented much higher activity than Au and alloying them the activity of Pd decreased significantly.

The co-operation of Au and Pd on an active TiO_2 support interacting strongly with Au is an intriguing study. For easier interpretation similar size of the components in the bimetallic and the monometallic references is required. This is why the method of adsorption from sols have been used for the preparation of the supported bi- and monometallic nanoparticles that provides an efficient control of particle size and size distribution [15,16].

In the study of heterogeneous catalysts X-ray absorption spectroscopy (XAS) is now widely recognized to describe the local order around metal elements [17–19] even for nanometer scale metallic clusters [20,21]. In the present paper we report in situ XAS characterization of a TiO_2 supported bimetallic AuPd system correlated with X-ray diffraction (XRD) measurements, transmission electron microscopy (TEM), CO chemisorption and with the catalytic activity measured in the CO oxidation.

2. Experimental

2.1. Sample preparation

For sol preparation $HAuCl_4 \times 3H_2O$ and $PdCl_2$ were used as precursors, tannin and tri-Na-citrate-2-hydrate as reducing agent and stabilizer simultaneously, distilled water served as solvent. The aqueous solution of the Au and Pd precursors was mixed with the solution of tannin and sodium-citrate, whose pH was set to 7.5 by adding 1 wt.% sodium carbonate solution. The sol formation was allowed to proceed at 65 °C under vigorous stirring. During the reduction process the color of the solutions changed from yellow to deep brown and red for Pd and Au, respectively, and suddenly to deep brown for the bimetallic samples. The detailed parameters of the preparation of sols (including several parallel experiments) with the mean particle sizes and the standard deviation of the sizes are presented in Table 1.

SAu2, SPd2 and SAuPdS2 sols were adsorbed on TiO_2 (P-25, Degussa) producing samples designated by TSAu2, TSPd2 and TSAuPdS2, respectively. For the sake of a more efficient adsorption of the metal nanoparticles the pH of the solutions was decreased to about pH = 2 by adding 1N HNO_3 prior to suspending

Table 1
Parameters of sol preparation

Sample	$[Au^{3+}]$ (mM)	$[Pd^{2+}]$ (mM)	Reducing agent/stabilizer concentration (wt.%)		d_{TEM} (nm)	σ_d (nm)
			Na-citrate	Tannin		
SAu1	0.25	–	0.04	0.01	6.1	1.2
SAu2					7.3	2.6
SAu3					6.3	1.9
SPd1	–	0.20	–	0.03	4.8	2.4
SPd2					4.2	1.2
SAuPdS1	0.25	0.25	0.12	0.03	4.2	0.7
SAuPdS2					4.3	0.9

TiO_2 in the sols. The suspensions were stirred vigorously at room temperature for about 1 h, then TiO_2 was allowed to sediment, the liquid was decanted, the solid phase was dried for 2 days at 50–60 °C, and homogenized (in the case of the bimetallic sample the suspension had to be centrifuged for the separation of the liquid and the solid phase). The adsorption of the metal particles was not complete as it was indicated by the remaining pale color of the liquid phase.

2.2. Sample characterization

2.2.1. Transmission electron microscopy (TEM)

The metal content of the samples was determined by X-ray fluorescence (XRF) method. The particle size of the sols and the supported samples was determined by a Philips CM20 transmission electron microscope (TEM) operating at 200 kV. The sols or aqueous suspension of the supported samples were dropped on carbon-coated grid and after evaporating the water electron micrographs of the particles were taken. The particle size distribution was obtained by measuring more than 100 individual metal particles for sols, more than 50 for supported samples.

2.2.2. X-ray diffraction (XRD)

By X-ray diffraction (XRD) the crystalline phases were studied in the "as prepared" and calcined/reduced (400 °C/5% O_2 in He/1 h followed by 200 °C/H_2/1 h) state of the supported samples. The crystallite size was determined on the basis of the Sherrer equation. The molar composition of the bimetallic phases was estimated from the lattice parameter shift calculated from the angular position of the metal reflections using the Vegard's law.

2.2.3. X-ray absorption spectroscopy (XAS)

XAS experiments were performed on the "as prepared" TSAuPdS2 sample using DCI storage ring operated with electron energy of 1.85 GeV and a current between 260 and 360 mA. Data were collected using a double crystal Si(1 1 1) monochromator for the Au L_{III} edge (11,919 eV) and Ge(4 0 0) for the Pd K-edge (24,350 eV) and a double mirror in borosilicate for the rejection of harmonics. At Pd K-edge the transmission mode while at the Au L_{III} edge the fluorescence mode were used. The normalised EXAFS spectra were isolated from the experimental data using standard procedure [22]. Data analysis was performed with the use of the "EXAFS pour le Mac" package [23]. Fourier transforms (FT) of the k^3 weighted EXAFS functions were obtained using a Kaiser type window ranging from 3.0 to 12.0 $Å^{-1}$ beyond the Au L_{III} edge (from 2.5 to 6.0 $Å^{-1}$ beyond the Pd K-edge). In this work all FT are calculated and presented without a phase correction. The inverse Fourier transforms (filtered EXAFS) were then obtained in the range between 1.71 and 2.68 Å for Au (between 1.59 and 2.85 Å for Pd).

Gold and palladium metallic foils were employed as references for the Au–Au and Pd–Pd bonds [24]. Regarding the Au–Pd and Pd–Au bonds Pt–Pd alloy has been used. A two-shell least-squares fitting procedure (in k space) using the single scattering EXAFS formulation was used to extract the co-ordination number (N), distance (R), and Debye–Waller factor ($\Delta\sigma$). Numerical simulation corresponds to a typical residual equal to 10^{-2}. For all simulations, the edge shift ΔE was maintained at a value less than 4 eV [25]. The uncertainty in the co-ordination numbers (ΔN) is usually less than 20%. Following standards and criteria in XAS [26], the error bars on fitted parameters can be estimated by using standard statistical procedure [27]. The uncertainty for ΔN is lower than one, which is more important than the mean standard deviation in $\chi(k)$ using the statexafs code [28].

2.2.4. CO chemisorption and CO oxidation

CO chemisorption was applied to measure the accessible Pd surface. The chemisorption was carried out in a pulse flow system equipped with QMS and TCD. The 5% CO/He pulses were introduced at room temperature after heating the sample in 5%O_2/He at 400 °C for 1 h (the CO_2 and CO evolution during the heating up period of calcination were recorded by QMS) followed by reduction in hydrogen at 200 °C for 1 h.

The catalytic activity of the calcined/reduced samples was tested in CO oxidation in a plug flow reactor operating at atmospheric pressure under differential regime, the product was analyzed by gas chromatograph equipped with TCD detector. The composition of the reaction mixture was 5.6 mbar CO and 91.8 mbar O_2 in He, the temperature was 60 °C.

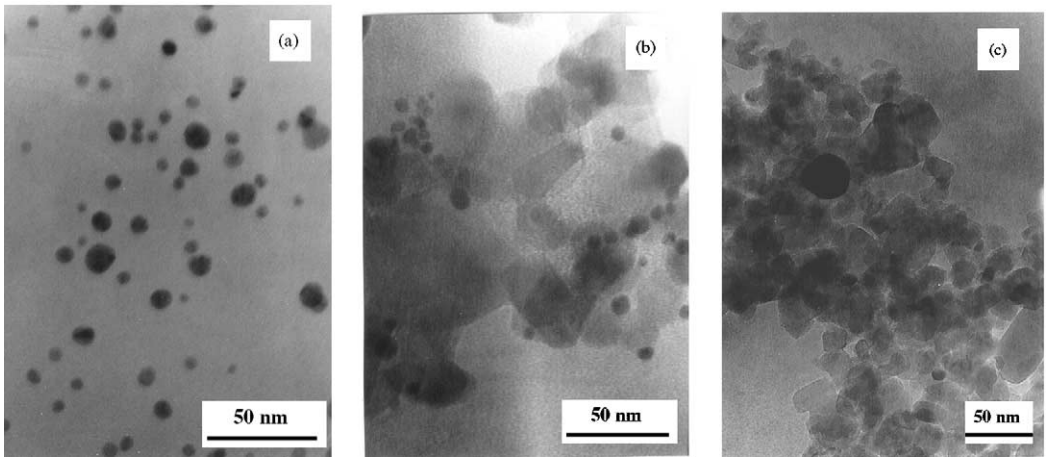

Fig. 1. TEM pictures of Au sol and the TiO_2 supported sample: (a) SAu2 sol; (b) "as prepared" TSAu2; and (c) calcined/reduced TSAu2.

3. Results

In the preparation of Au–Pd bimetallic as well as gold and palladium nanoparticles with narrow size distribution the parameters were changed to find the optimal conditions. In Table 1 the particle size of the different metal sols produced in selected way by two to three parallel preparations and measured by TEM are presented. As can be seen the size in the three types of sols is quite similar to each other and varies between 4.2 and 7.3 nm. On the other hand, the reproducibility of sol preparation concerning the particle size and the size distribution is satisfying. The extent of adsorption of the original sols on TiO_2 was not sufficient, therefore we changed the surface charge of the support by decreasing the pH from the original pH = 5–6 to pH = 2, in which case the liquid phase quickly leached and the solid darkened indicating the increased metal sol adsorption. The size of the metal particles during the adsorption process remained the same. In Fig. 1 typical TEM pictures of Au sol and the TiO_2 supported sample: (a) SAu2 sol; (b) "as prepared" TSAu2; and (c) calcined/reduced TSAu2 are presented. For TSAu2 the mean particle diameter in the as prepared state (6.9 ±

Table 2
Metal loading, crystalline phases, particle size and the estimated concentration of surface metal atoms in the supported samples

Sample	As prepared state			Calcined/reduced state			
	Au (wt.%)	Pd (wt.%)	XRD phases (size in nm)	XRD phases[a] (size in nm)	d_{TEM} (nm)	$M_{surface,TEM}$ (μmol g_{cat}^{-1})	$Pd_{surface,CO}$[b] (μmol g_{cat}^{-1})
TSAu2	1.95	–	Au (8)	Au (8)	12.9 ± 5.9	9.0/Au	–
TSPd2	–	1.10	Pd (≤4)	Pd (8)	8.8 ± 3.6	13.2/Pd	18.8
TSAuPdS2	1.08	0.55	Au75Pd25 (5)	Au75Pd25 (8)	9.6 ± 4.0	6.2/Pd, 6.5/Au	17.0
Au/SiO_2[c]	0.73	–	–	Au (32)	95.1 ± 28.7	0.46/Au	–
Pd/SiO_2[c]	–	1.53	–	PdO (10) 98% Pd (40) 2%	9.2 ± 3.6	17.5/Pd	16.7
$50Au50Pd/SiO_2$[c]	0.63	0.65	–	PdO (9) 19% Au52Pd48 (4) 81%	6.2 ± 2.1	11.1/Pd 5.8/Au	10.1

[a] XRD was measured on the calcined form of the SiO_2 supported samples.
[b] Concentration of surface Pd atoms calculated from CO chemisorption; no CO chemisorption was detected on the monometallic Au samples.
[c] The data are taken from [14].

2.8 nm) agrees well with that characteristic of the precursor sol (see Table 1). Several properties of the supported samples are presented in Table 2. As a comparison the corresponding data of SiO_2 supported Au, Pd and AuPd (reported in [14]) are inserted, as well.

Organic residues contaminate the supported samples to a large extent. In order to remove them the samples were pretreated before catalytic tests by calcination at 400 °C for 1 h in O_2/He mixture, which treatment causes the oxidation of Pd [29]. The calcined samples were reduced in H_2 at 200 °C. These treatments resulted in sintering the metal particles, the particle diameters doubled and the size distribution widened in all three samples. TEM micrographs (e.g. Fig. 1(c)) show predominantly spherical particles, whose mean particle diameters are close to the crystallite sizes determined by XRD. The latter shows about $Au_{75}Pd_{25}$ molar composition for the bimetallic crystallites both in the as prepared and in the calcined/reduced form, but crystalline monometallic or oxide phases were not detected. However, on the basis of the metal loading measured by XRF the molar ratio is Au/Pd = 1. According to this twice as much Pd as is present in the bimetallic crystallites, must be invisible for XRD.

In Fig. 2 the XANES part of the absorption spectrum of the "as prepared" TSAuPdS2 is presented

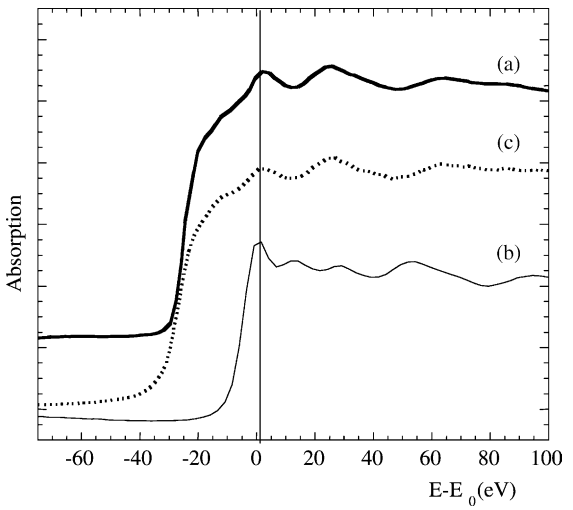

Fig. 2. Comparison of the XANES spectra of the metallic Au foil at Au L_{III} edge (a); PtPd alloy at Pt L_{III} edge (b); and AuPd/TiO_2 at Au L_{III} edge (c).

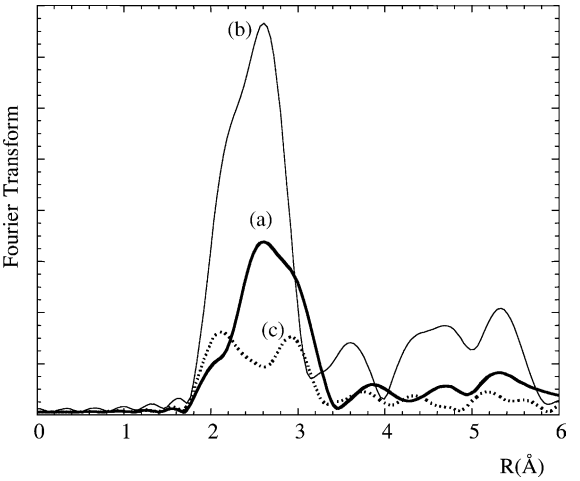

Fig. 3. Comparison of the FT modules between the absorption spectrum of metallic Au foil at Au L_{III} edge (a); PtPd alloy at Pt L_{III} edge (b); and AuPd/TiO_2 at Au L_{III} edge (c).

which resembles closely to that recorded on Au metallic foil. However, the FT module (Fig. 3) beyond the Au L_{III} edge confirm that in the first co-ordination sphere of Au atoms both Au and Pd atoms are present. More precisely, numerical simulations of the EXAFS oscillations (Table 3) points out the presence of some heteroatomic Au–Pd bonds inside the catalyst. Regarding the Pd K-edge the same approach has been performed. If we consider the FT module (Fig. 4), it seems that the first co-ordination sphere of palladium atoms contains several kinds of atoms. More

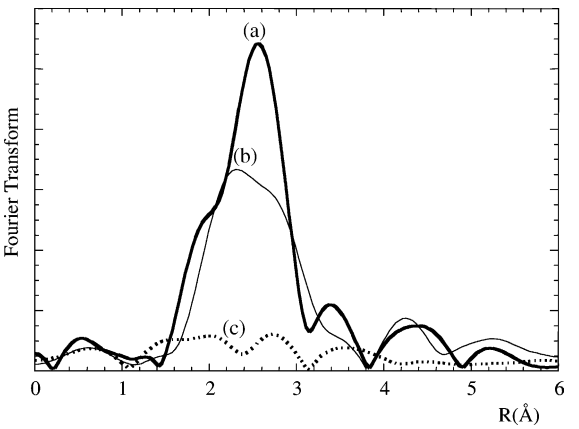

Fig. 4. Comparison of the FT modules between the absorption spectrum of metallic Pd foil (a); PtPd alloy (b); and AuPd/TiO_2 (c) at Pd K-edge.

Table 3
Structural parameters associated to the EXAFS analysis of the TiO_2 supported bimetallic sample performed at the Au L_{III} edge and at the Pd K-edge

TSAuPdS2					
N_{AuAu}	R_{AuAu} (Å^{-1})	$\Delta\sigma_{AuAu}$ (Å^{-1})	N_{AuPd}	R_{AuPd} (Å^{-1})	$\Delta\sigma_{AuPd}$ (Å^{-1})
9.5	2.84	0.04	1.9	2.82	0.02
N_{PdPd}	R_{PdPd} (Å^{-1})	$\Delta\sigma_{PdPd}$ (Å^{-1})	N_{PdAu}	R_{PdAu} (Å^{-1})	$\Delta\sigma_{PdAu}$ (Å^{-1})
1.1	2.83	0.00	1.2	2.76	0.02
N_{PdO}	R_{PdO} (Å^{-1})	$\Delta\sigma_{PdO}$ (Å^{-1})			
1.4	2.06	0.03			

precisely, palladium, gold as well as oxygen atoms are present in the local environment of palladium. Numerical simulations are presented in Table 3.

From the particle diameter one can estimate the metal dispersion based on the following relations: $D = 1.12/d$ for Pd; $D = 1.17/d$ for Au, where d is the particle diameter (in nm) and D is dispersion. In the case of TSAuPdS2 $d \times D = 1.145$ factor was applied as a weighted average value of the monometallic systems. Table 2 contains the concentration of the surface metal atoms determined from the dispersion data.

For calculation of the number of exposed Pd atoms from CO chemisorption the Pd/CO stochiometry should be known. It varies between 1 and 2 depending on the relative concentration of the linear and bridged form that is reflected in the relative intensity of the corresponding IR absorbance bands. However, the exact ratio can hardly be determined because of the lack of the exact extinction coefficients. The relative amount of linear and bridged CO is typically increases when concentration of Pd decreases in bimetallic particles [29–32]. For the calculation of number of surface Pd atoms we used CO/Pd = 1.5 for the titania supported monometallic and CO/Pd = 1 for the bimetallic sample. As can be seen in Table 2 smaller amount of surface Pd is estimated from TEM data, that may be explained by the presence of small particles not visible by TEM, and by the possible difference between the surface and the bulk composition in the bimetallic sample.

Table 4 illustrates the results of the CO oxidation tests for the TiO_2 supported and the analogous SiO_2 supported systems. Silica supported samples produce activity of same order of magnitude as titania supported ones at about 80 °C higher temperature, in the case of monometallic Au at about 160 °C higher

Table 4
Catalytic activity in CO oxidation reaction (for titania supported samples 5.6 mbar CO + 91.8 mbar O_2 in He, for silica supported ones 4.5 mbar CO + 5.0 mbar O_2 in He reaction mixture was applied)

Sample	Temperature (°C)	Initial reaction rate (μmol min^{-1} g_{cat}^{-1})	TOF_{XRD}[a] (min^{-1})	TOF_{TEM}[a] (min^{-1})	TOF_{CO}[b] (min^{-1})
TSAu2	60	12.1	0.84	1.35	–
TSPd2	60	13.7	0.95	1.04	0.73
TSAuPdS2	60	22.9	–	–	–
Au/SiO_2[c]	220	0.16	–	0.36	–
Pd/SiO_2[c]	140	9.3	0.59	0.53	0.56
$50Au50Pd/SiO_2$[c]	140	3.6	0.24[d]	0.32[d]	0.36[d]

[a] Reaction rate referred to one surface metal atom (μmol CO_2/min/μmol M_s), the amount of Au_s was calculated by $D \times Au_{total}$, where $D = 1.17/d$, the amount of Pd_s was calculated by $D \times Pd_{total}$, where $D = 1.12/d$ (D: dispersion; d: particle diameter (in nm) measured by XRD or TEM).

[b] Reaction rate referred to one surface Pd atom (μmol CO_2/min/μmol Pd_s), the amount of Pd_s was calculated by $D \times Pd_{total}$, where D was estimated from CO chemisorption assuming different CO/Pd stochiometry.

[c] The data are taken from [14].

[d] TOF related to one surface Pd atom, since surface Au has no activity at 140 °C.

temperature. The specific initial reaction rates of TSAuPd2 (referred to 1 g of catalyst) is about twice as high as that of the titania supported monometallic samples. The TOF values of the Pd/TiO_2 and Au/TiO_2 systems referred to one surface metal atom (determined on the basis of mean particle size), are similar. For Au/SiO_2 80 °C higher reaction temperature is required to reach similar activity as Pd/SiO_2. The activity of the silica supported bimetallic catalyst is ca. half of that of monometallic palladium sample.

4. Discussion

According to the literature data activity of gold can be increased by addition of noble metals [33–37]. Regarding the Pd–Au bimetallic system, several studies have already been published [14,29,38–40]. For example, Liu et al. [38] have characterized the system by TEM, XRD and XPS to elucidate the formation of bimetallic colloids. XPS data indicated that the constituent elements were in metallic state and that palladium atoms were concentrated on the surface of the alloy.

Regarding our $AuPd/TiO_2$ catalyst, the XAS underlines the presence of Au–Pd bonds, pointing out the existence of an alloy inside the catalyst. The complete set of results seems to indicate that several phases may exist. We cannot exclude the presence of monometallic clusters and the presence of PdO like clusters, either. EXAFS being insensitive of poly-dispersion leads to the fact that we have no possibility to give either an average size for the metallic clusters or the distribution of the atoms inside the bimetallic particles. Nevertheless, the presence of Pd–O bonds seems to indicate palladium atoms being at the surface of the cluster. As a complementary technique, XRD clearly supports the presence of bimetallic phases with a particle size as low as a few nanometers.

The studied TiO_2 supported monometallic Au and Pd nanoparticles show similar TOF in the CO oxidation. In the literature TOF = 0.6 min^{-1} at 0 °C [13], TOF = 5.0–0.08 min^{-1} at 40 °C [41] were reported for Au/TiO_2 containing similar size Au particles as TSAu2. On the calcined and low temperature (473 K) reduced TSAu2 sample the residual chloride content might diminish the catalytic activity [41]. The activity of Pd/TiO_2 is in the same order of magnitude as reported in [42]. The specific activity of the bimetallic sample is almost twice as high as that measured for monometallic catalyst. If we assume that Pd and Au atoms keep their identity and catalytic activity in the bimetallic system, the specific activity of the $PdAu/TiO_2$ sample can be estimated by the sum of $TOF_{Au} \times N_{Aus} + TOF_{Pd} \times N_{Pds}$, where N_{Aus} and N_{Pds} are the number of surface Au and Pd atoms in 1 g of the bimetallic sample, respectively. The values are 13.6, 15.2 and 22.1 μmol min^{-1} g_{cat}^{-1}, when the dispersion calculated from crystallite size (XRD), particle size (TEM) and CO chemisorption (except Au_s) is applied to determine the number of surface atoms, respectively. These values are somewhat lower than the experimentally measured 22.9 μmol min^{-1} g_{cat}^{-1} activity of TSAuPdS2, thus, only slight synergism exists in the CO oxidation. Despite the uncertainty, the three methods complement each other quite well. Since the TOF values of the monometallic samples are nearly identical, the presence of some segregation would not affect significantly the above calculations. Thus we can establish that the activity of the bimetallic system is close to or somewhat higher (maximum two times) than the sum of the activity of corresponding monometallic Au and Pd sufaces on TiO_2 support. This result differs from that experienced on SiO_2 supported AuPd bimetallic systems, at which alloying decreased the catalytic performance of the higher activity Pd/SiO_2 (see Table 4). In the silica supported system it could be tentatively attributed to (i) chemical effect, since in the bimetallic particles the formation of surface Pd-oxide layer is inhibited; (ii) geometric effect, the decreasing population of Pd ensembles, which might provide side by side activation of CO and O_2; and (iii) electronic effect [14]. The former two effects can be resulted in the hindrance of O_2 activation on Pd, which may manifest itself in decreasing activity. In the TiO_2 supported system the activated oxygen supposedly can be produced on the support as well, so the alloying do not cause the degradation of the activity.

5. Conclusions

Monometallic Au, Pd and bimetallic AuPd nanoparticles were prepared by sol technique and deposited on TiO_2 support. The stable metal sol of narrow size distribution was characterized by TEM. After removing

the stabilizer from the supported samples by TPO the original particle size (4–7 nm) increased to 9–13 nm in diameter.

Presence of bimetallic particles was confirmed by in situ EXAFS at Au L_{III} and Pd K-edges as well as XRD experiment.

In the CO oxidation reaction the catalytic activity of the bimetallic $AuPd/TiO_2$ seems to be equal to or somewhat higher than the sum of the activity of monometallic analogous weighted according to the estimated surface of Au and Pd in the bimetallic system.

Acknowledgements

The authors are indebted to the National Science and Research Fund (OTKA grant #T-034920) for financial support and to the COST D15/005/99 and D15/016/00 projects.

References

[1] P. Chakraborty, J. Mater. Sci. 33 (1998) 2235.
[2] K. Fukumi, A. Chayahara, K. Kodano, T. Sakaguchi, Y. Horino, M. Miya, K. Jujii, J. Hayakawa, M. Satou, J. Appl. Phys. 75 (1994) 3075.
[3] J.R. Mellor, A.N. Palazov, B.S. Grigorova, J.F. Greyling, K. Reddy, M.P. Letsoalo, J.H. Marsh, Catal. Today 72 (2002) 145.
[4] M. Haruta, M. Daté, Appl. Catal. A 222 (2001) 427.
[5] M. Haruta, Catal. Today 36 (1997) 153.
[6] D. Guillemot, M. Pollisset-Thfoin, D. Bonnin, D. Bazin, J. Fraissard, J. Phys. C2 (1997) 931.
[7] D. Andreeva, T. Tabakova, V. Idakiev, P. Christov, R. Giovanol, Appl. Catal. A 169 (1998) 9.
[8] G.H. Takaoka, T. Hamano, J. Matsuo, I. Yamada, K. Fukushima, NIM B 121 (1997) 503.
[9] S. Naito, M. Tanimoto, J. Chem Soc. Chem. Commun. 832 (1988).
[10] F. Boccuzzi, E. Guglielminotti, F. Pinna, G. Strukul, Surf. Sci. 377–379 (1997) 728.
[11] R.E. Benfield, D. Grandjean, M. Kroll, R. Pugin, T. Sawitowski, G. Schmid, J. Phys. Chem. B 105 (2001) 1961.
[12] H. Liu, A.I. Kozlov, A.P. Kozlova, T. Shido, K. Asakura, Y. Iwasawa, J. Catal. 185 (1999) 252.
[13] M. Haruta, S. Tsubota, T. Kobayashi, H. Kageyama, M. Genet, B. Delmon, J. Catal. 144 (1993) 175.
[14] K. Frey, D. Horváth, Zs. Koppány, A. Beck, V. La Parola, L.F. Liotta, G. Pantaleo, A.M. Venezia, L. Guczi, to be published.
[15] J.-D. Grunwaldt, C. Kiener, C. Wögerbauer, A. Baiker, J. Catal. 181 (1999) 223.
[16] A. Horváth, A. Beck, Zs. Koppány, A. Sárkány, L. Guczi, J. Mol. Catal. A 182–183 (2002) 295.
[17] T. Shido, R. Prins, Curr. Opin. Solid State Mater. Sci. 3 (1998) 330.
[18] A.Y. Stakheev, L.M. Kustov, Appl. Catal. A 188 (1999) 3.
[19] K.J. Chao, A.C. Wei, J. Elec. Spec. Rel. Phen. 119 (2001) 175.
[20] D. Bazin, D. Sayers, J. Rher, J. Phys. Chem. B 101 (1997) 11040.
[21] D. Bazin, L. Guczi, Recent Res. Dev. Phys. Chem. 3 (1999) 387.
[22] D.E. Sayers, B.A. Bunker, in: D.C. Koningsberger, R. Prins (Eds.), X-ray Absorption: Principles, Applications, Techniques of Exafs, Sexafs and Xanes, Wiley, New York, 1998, p. 211.
[23] A. Michalowicz, Ph.D. thesis, University of Val de Marne, 1990.
[24] A. Khodakov, J. Lynch, D. Bazin, B. Rebours, N. Zanier, B. Moisson, P. Chaumette, J. Catal. 68 (1997) 16.
[25] A. Michalowicz, G. Vlaic, J. Synch. Rad. 5 (1998) 1317.
[26] F.W. Lytle, D.E. Sayers, E.A. Stern, Physica B 158 (1989) 701.
[27] P.R. Bevington, Data Reduction and Error Analysis for the Physical Sciences, McGraw-Hill, New York, 1992, p. 205.
[28] J.Ph. Piquemal, C. Leroy, A. Michalowicz, unpublished program available on the LURE, http://www.lure.u-psud.fr, 1999.
[29] A.M. Venezia, V. La Parola, G. Deganello, B. Pawelec, J.L.G. Fierro, J. Catal. 215 (2003) 317.
[30] Y. Soma-Noto, W.M.H. Sachtler, J. Catal. 32 (1974) 315.
[31] E.L. Kugler, M. Boudart, J. Catal. 59 (1979) 201.
[32] E.A. Sales, J. Jove, M.J. Mendez, F. Bozon-Verduraz, J. Catal. 195 (2000) 88.
[33] C. Montassier, J.C. Ménézo, J. Naja, J. Barbier, J.M. Dominguez, P. Sarrazin, B. Didillon, J. Mol. Catal. 91 (1994) 107.
[34] M. Wolf, H. Knözinger, J. Mol. Catal. 25 (1984) 273.
[35] J.K.A. Clarke, A.C.M. Creaner, T. Baird, Appl. Catal. 9 (1984) 85.
[36] J. Barbier, P. Marécot, G. Del Angel, P. Bosch, J.P. Boitiaux, B. Didillon, J.M. Dominguez, I. Schiftef, G. Espmos, Appl. Catal. A 116 (1994) 179.
[37] T. Galo Cárdenas, D. Rodrigo Segura, Mater. Res. Bull. 35 (2000) 1369.
[38] H. Liu, G. Mao, S. Meng, J. Mol. Catal. 74 (1992) 275.
[39] M. Bonarowska, J. Pielaszek, W. Juszczyk, Z. Karpinski, J. Catal. 195 (2000) 304.
[40] M. Bonarowska, J. Pielaszek, V.A. Semikolenov, Z. Karpinski, J. Catal. 209 (2002) 528.
[41] S.D. Lin, M. Bollinger, M.A. Vannice, Catal. Lett. 17 (1993) 245.
[42] S.N. Pavlova, V.A. Sadykov, N.N. Bulgakov, M.N. Bredikhin, J. Catal. 161 (1996) 517.